(NASA TMX-50380)

X63 15494

CODE-2A

37 p.

ANALOG SIMULATION OF PILOTED EARTH REENTRY AT PARABOLIC VELOCITY

By M. T. Moul, E. J. White, and A. A. Schy [1963] 37 p. 6 refs

NASA Langley Research Center
Langley Station, Hampton, Va., U.S.A.

Presented at International Symposium on Analogue and Digital Techniques Applied to Aeronautics

Conf

Liege, Belgium
September 9-12, 1963

ANALOG SIMULATION OF PILOTED EARTH REENTRY AT PARABOLIC VELOCITY

By M. T. Moul,* E. J. White,** and A. A. Schy*

NASA Langley Research Center

SUMMARY

Piloted earth reentry at parabolic velocity was satisfactorily simulated by employing analog computing equipment. The ability of a pilot to control a spacecraft and to perform long- and short-range navigation tests was determined. In simulated emergency conditions the pilot accomplished a safe entry with a display presentation of only bank angle and longitudinal acceleration.

INTRODUCTION

For several years now the problems associated with the earth entry of spacecraft returning from extraterrestrial flight have been under study. Three main problems to be contended with for survival in such an entry are (1) acceleration environment, (2) aerodynamic heating, and (3) planetary capture. Solutions for safe atmospheric entry are accomplished by suitable trade-offs between vehicle design and reentry trajectories. One treatment of this subject has been presented by Chapman in reference 1.

The limiting entry trajectories are shown in figure 1. Shallow entry is restrained by the requirement of earth capture, whereas steep entry is restrained by acceleration or heating environment. By definition an entry more shallow than the overshoot condition would result in return to orbit. Likewise, an entry steeper than the undershoot condition would encounter intolerable accelerations or heating.

From such possible entry conditions a maneuverable reentry vehicle by utilizing its aerodynamic capability possesses some range-control potential. Some possible trajectories that a controlled lifting spacecraft might traverse are also shown in this figure. The short range entries result from pulling down into a high g condition from either a shallow or steep entry. The long range entries result from producing a controlled skip to a given altitude followed by a suborbital glide at $(L/D)_{max}$. A study of flight mechanics and range-control capabilities for several classes of reentry vehicles is presented in reference 2.

Inasmuch as the accessible landing area designated by the arrows depends on the ability to control the spacecraft along the extreme trajectories, a fixed-base

---

*Aerospace Engineers.

**Aerospace Physicist.

simulation was undertaken to determine the pilots' capabilities in this respect. It was desired to investigate the effects of loss of automatic damper equipment on the pilot's ability to perform the maneuvers required in the extreme trajectories. This ability could be evaluated in a qualitative manner by simply noting whether the pilot could maintain control of the vehicle with the dampers out and by comparing time histories for damper-in and damper-out conditions. As a rough quantitative measure of this ability, a comparison was made of r.m.s. deviations in final range for series of entries with dampers in and out. For this purpose, it was particularly important to have the computed range reasonably accurate even on long range entries and it was also important to have an accurate short-period, dynamic representation of the undamped vehicle throughout the trajectory. This combination of requirements, along with the necessity for real-time computation with the human pilot in the loop, gave rise to unusual difficulties in attaining a satisfactory analog setup. Both the analog programing techniques and the experimental results of the simulation will be discussed herein.

SIMULATION REQUIREMENTS

The problem posed in the introduction is basically one of pilot control of spacecraft position and attitude over a wide range of altitude and velocity. The primary elements of the simulation are then (1) an electronic computer solving a set of six-degree-of-freedom equations of motion, (2) a pilot station including controllers that provide a means for controlling attitude (propulsive systems for controlling velocity are excluded), and (3) an information display of trajectory, dynamic, and acceleration parameters.

No automatic guidance systems are included; navigational tasks are accomplished by the pilot closing the loop between output quantities and control elements by the use of the information display and spacecraft controllers.

The required ranges of some of the variables, which were considered to present analog programing problems, are as follows:

Time	0 to 20 min
Altitude	100,000 to 400,000 ft
Atmospheric density	3×10^{-5} to 7×10^{-8} slug/cu ft (lb-sec^2/ft^4)
Velocity	14,000 to 36,000 ft/sec
Acceleration	0 to 320(10g) ft/sec^2
Dynamic pressure	0 to 700 lb/ft^2
Angle of attack	0 to 50°
Angle of bank	±720°

Particularly critical areas of the computer program, where accuracy must be maintained, were foreseen to be in the generation of linear accelerations and dynamic pressure. Accuracy is required in linear accelerations in order for the trajectories $\left(\iint a\, dt\right)$ to be meaningful. In particular, vertical accelerations are important in the long-range skipping trajectories where consistent range data

are required. In this condition the net vertical acceleration, although near zero, is an important factor in determining the maximum altitude and range traveled in the skipping trajectory. Another variable affecting the trajectory is dynamic pressure. Dynamic pressure is an important variable in determining the aerodynamic forces (lift and drag) which influence accelerations and consequently the trajectory.

One purpose of this investigation was to determine the ability of a pilot to control the vehicle and accomplish a given task in the vehicle condition of no damping augmentation, for which the spacecraft is neutrally stable. The simulation of this condition requires nonlinear equipment of sufficient dynamic performance that no appreciable phase lags are encountered in the vehicle dynamics loops. The existence of phase lags could produce divergent characteristic modes in the no-damping condition rather than the desired near-neutral stability.

The control of vehicle dynamics and trajectory in such a condition is a marginal situation in that the pilot must share his attention between the two tasks. Any decrease in damping may produce a situation in which the pilot loses control of either vehicle attitude or trajectory. Obviously then, an accurate dynamic simulation is required in order to obtain valid results in the investigation.

The requirements for accurate trajectory data and vehicle dynamics led to the choice of the following axes systems for defining the vehicle motion:

(1) Rotational degrees of freedom - a body axes system with X-axis coinciding with the spacecraft axis of symmetry

(2) Translational degrees of freedom - a moving set of axes fixed to the spacecraft center of gravity, the Z-axis directed along the local vertical, and the X-axis directed along the horizontal component of the initial velocity vector, designated a geographic axes system

The selected geographic system was appropriate for this problem, since the earth was assumed to be spherical and nonrotating. Hence, the orientation of the specific trajectory to the earth polar axis was not required. The axes systems, equations of motion, and analog programing techniques for this type of problem are discussed in detail in references 3 and 4. The axes system selected for this problem is the same as one discussed in reference 3. Since motion of translation was computed in a local horizontal axes system, aerodynamic forces were determined in the vehicle body axes system and then transferred to the geographic set by direction cosines expressed in terms of the Euler angles relating the two sets of axes. Definitions of the forces, angles, and other physical parameters are given in appendix A; the equations of motion for the selected axes systems are given in appendix B.

Vehicle Description

The spacecraft configuration considered in this study is shown in figure 2. It is a blunt-face capsule and is trimmed to a constant lift-drag ratio of 0.5 by means of center-of-gravity offset in the vertical direction. The spacecraft

possesses static aerodynamic stability, and trajectory control is accomplished by controlling bank angle by which the lift vector can be directed upward, downward, or to either side.

Aerodynamic Representation

Aerodynamic forces and moments were expressed in the body axes system, with wind-tunnel tests and theory indicating that

(1) C_{Z_α}, C_{Y_β}, C_{n_β}, C_{l_β}, C_{l_p}, C_{m_q}, C_{n_r} were constant and

(2) C_m and C_X were functions of angle of attack (as shown in fig. 2).

Control Systems

Proportional reaction controls were provided about all three axes. Within the atmosphere three axes damping augmentation using simple rate damping was applied through the reaction controls. Pilot controllers were provided for all three axes; however, pitch and yaw controllers were used by the pilot only in space environment to control attitude or in the atmosphere to damp vehicle oscillations in simulated conditions of damper failure.

Pilot Station and Display Instrumentation

Figure 3 is a sketch of the simulator equipment - the instrument panel, pencil-type controller at the right hand, foot pedals, pilot seat, and an X-Y plotter. The hand controller permits proportional control of motions about the vehicle axis of symmetry (roll) by left and right stick deflections and about the transverse (pitch) axis by fore and aft stick deflections. The foot pedals allow proportional control of yawing (left and right) motions.

Flight data displayed on the main instrument panel are, on the top row, time, vehicle velocity, vehicle angular velocities (p, q, and r), flight-path heading angle A, and crossrange Y. On the middle row, the first two meters display normal acceleration a_n and dynamic pressure $\bar{q}$, respectively. The center instrument is a three-axis attitude indicator displaying ψ, θ, and ϕ on the ball and angles of attack α and sideslip β on two bar indicators in front of the ball. The two meters to the right of the attitude indicator display altitude h and rate of climb $\dot{h}$. On the bottom row are presented transverse acceleration a_y, resultant acceleration a_R, quickened resultant acceleration $\bar{a}_R$, and range. On the X-Y plotter at the pilot's left, vehicle trajectory is plotted to give the pilot a clear picture of his downrange position and altitude.

Above the main instrument panel an oscilloscope was mounted, on which a composite guidance and situation display was presented. The scope display was used for long range entries, in which the pilot could not be expected to perform the necessary control of skipping trajectories with the usual flight instruments.

Preliminary runs indicated that the desired skips could be performed by following a given program of climb rates. The desired climb rates were expressed as a function of axial acceleration and mechanized for presentation on the oscilloscope. Figure 4, a sketch of the scope face, shows the reference curve, with climb rate presented along the abscissa and axial acceleration along the ordinate. The actual trajectory condition was shown by a moving pip, and the pilot by controlling bank angle caused the pip to follow the reference curve. As a result of following this reference curve, a skip to an altitude of about 350,000 feet resulted.

To further aid the pilot, vehicle bank angle was added to the scope as a needle indicator corresponding to the roll attitude of the vehicle Z-axis. This modification improved the display by eliminating the time otherwise required in scanning from the oscilloscope to the attitude indicator.

DISCUSSION OF PROGRAMING TECHNIQUES

Although the programing techniques which are discussed herein do not necessarily represent completely new concepts in analog computer programing, it is felt that outlining these techniques is useful in indicating the extent of the simulation problem and the manner in which an existing facility might be utilized to solve such a problem. The analog computer capacity existing at the beginning of this simulation consisted of two small consoles with multipliers and resolvers which were electromechanical. This computer did not have automatic setup and readout equipment. During the early phases of this simulation a more modern computer (EAI-231-R) became available, at which time part of the computer program was transferred to it. This computer was equipped with electronic multipliers and automatic setup and readout equipment (ADIOS). After the facility expanded, the entire program was transferred to the more modern equipment.

Figure 5 shows a general block diagram of the six-degree-of-freedom reentry simulation, including cockpit. For simplicity, not all of the variables which are displayed to the pilot are shown on the diagram. This simulation requires approximately 300 operational amplifiers plus a large complement of nonlinear equipment. To minimize the daily checkout time, the automatic setup and readout equipment was used. This allowed complete static and dynamic checks to be performed daily. Each day two different dynamic checks were performed. The first was a complete six-degree-of-freedom response at an intermediate altitude where altitude rate was small. This was chosen to check the dynamic response of the computer. The second was a trajectory check where the problem ran until after vehicle pullout. This was used to check the long-time integration. These checks were compared to the same conditions done on the digital computer. All the instruments in the cockpit were monitored during the trajectory check to give assurance that they were operating properly. Using the automatic setup features of the computer, the entire setup time, including static and dynamic checks, required approximately 2 hours. Extensive checks of this nature could not have been performed daily with sufficient investigation time remaining in a normal 8- or 10-hour day without the aid of this automatic setup and readout equipment.

Loop Analysis

Digital solutions of the uncoupled longitudinal and lateral responses were obtained to be used as accuracy criteria. When only the electromechanical multipliers were used, the analog solutions did not agree with the digital solutions. The disagreement was due to errors in the analog solution caused by the poor dynamic response of the servomultipliers. The operating frequency of some of the variables approached 1 cycle per second. At this frequency enough phase shift was introduced by the servomultipliers to cause the solutions to diverge. For lightly damped conditions the analog solutions had extensive errors, doubling their amplitude in approximately three cycles. Since the simulation was restricted to real time, the difficulty could not be overcome by time scaling. If sufficient electronic multipliers had been available at the time, a remedy would have been to replace all the mechanical components by electronic components. However, only a limited number of the newly acquired electronic components did exist, and so it was necessary to perform a loop analysis to determine where it would be most advantageous to replace electromechanical components with electronic components. The discussion to follow points out the approaches in this analysis.

In the longitudinal investigation, as a result of linearization and the assumption that lateral variables were zero and linear velocities $\left(V_X \text{ and } V_Z\right)$ were constant, the problem was reduced to a consideration of the pitching-moment equation only. The pitching-moment equation thus becomes

$$I_Y\dot{q} = M_q q + (M)_\alpha + M_y$$

By assuming that the damping and control terms are equal to zero, the equation is further reduced to

$$I_Y\dot{q} = (M)_\alpha = \bar{q}SdC_m(\alpha)$$

which by virtue of the foregoing assumptions can be shown to be representative of a one-degree-of-freedom system possessing neutral oscillatory stability. Figure 6 shows the pitching-moment program, with all the servomotors in the loop as in the complete six-degree-of-freedom programing. The results were unstable. To further analyze the divergence, it can be assumed that $\alpha = \theta$; this assumption can be used to reduce the equation to

$$I_Y\dot{q} = \bar{q}SdC_m(\theta)$$

The new loop then becomes that shown by the dotted line from the θ integrator to the function generator. This eliminates all the servomotors from the loop except the one driven by q. This resulted in a neutrally stable response. The next step was to put everything back into the loop again, except the servoresolver from which α is obtained. This was accomplished by making a small

angle assumption for α, where $\alpha = w/u$. The division was made by using a time-division multiplier. (This small angle assumption was used for the loop investigation only.) The result was again divergent, which indicated one or all three of the other servos were at fault. It was found that by replacing the two servo-multipliers, which were driven by $\sin\theta$ and $\cos\theta$, with time-division multipliers the divergence was eliminated.

The same type of investigation was conducted for the lateral loop. However, here it was more difficult because there were two moment equations to consider. It was found that similar component substitutions were required for proper dynamic response.

Linear Acceleration Errors

Navigational errors were encountered because of the scaling required of the translational equations. The errors occurred because of the large ratios in maximum values of acceleration and velocity. For example, $\dot{V}_{x,max} \approx 400$ ft/sec^2, and $V_{x,max} \approx 40{,}000$ ft/sec, resulting in a ratio of 1 to 100. Since the equation must be scaled for V_x and solved for $\dot{V}_x$, this requires that the $\dot{V}_x$ terms be reduced appreciably by the coefficient potentiometers before being summed by the integrator. In some cases the acceleration voltage would be no greater than the noise level of the amplifier. These low signals being integrated over several hundred seconds produced intolerable errors in velocity and displacement. This was even more pronounced in the $\dot{V}_z$ equation during vehicle pullout and peak altitude after the pullout where the acceleration depended completely on the difference of gravity and the centrifugal force terms. A remedy for this difficulty is to decrease the gain at the input of the integrator. The method used to decrease this gain was to put an additional 1 μf capacitor in the feedback of the integrator and then take advantage of the 2 to 1 slow feature of the computer. This decreases the gain of the integrator by a factor of 4, which allows an increased voltage signal at the input of the integrator. For the $\dot{V}_x$ equation another factor of 3 was gained by perturbing the equation in addition to using the extra capacitors in the feedback. Since V_x is always positive and for most studies never drops below 14,000 ft/sec, the relationship may be written as

$$V_x = V_{x,o} + \Delta V_x$$

where $V_{x,o} = 27{,}000$ ft/sec and ΔV_x ranges from 13,000 ft/sec to -13,000 ft/sec. Perturbation of V_z and V_y provided no advantage since their positive and negative maximum values are equal.

Dynamic-Pressure Programing

Since the trajectory of the vehicle is very sensitive to the dynamic pressure $\bar{q}$ through the lift and drag forces, it is essential to get the best scaling

possible for $\bar{q}$. The straightforward method of generating $\bar{q}$ (multiplying $\frac{1}{2}\rho$ by V^2) gives a maximum voltage of less than 3 volts. Two or three programing alternates can be adopted to improve this resolution. Figure 7 shows a combination of programing methods which improves the scaling considerably. Since $\rho^{1/2}$ has a smaller variation than ρ over a given range of altitude, better scaling was obtained by forming $\rho^{1/2}V$ and then squaring the product to form $\frac{1}{2}\rho V^2 = \bar{q}$. In addition to this, the function $\rho^{1/2}$ can be more accurately formed by generating only the deviation from a straight line $\Delta\rho^{1/2}$ on the function generator. Since

$$\rho^{1/2} = \Delta\rho^{1/2} + ah + b$$

the major contribution is obtained from linear equipment. This method resulted in better scaling and accuracy for $\bar{q}$.

Dynamic Checks

After these programing techniques were applied, satisfactory dynamic checks were obtained. Figures 8(a) and 8(b) show the comparison of the analog and digital results. Figure 8(a) compares time histories of pitch, roll, and yaw rates for the combined longitudinal and lateral response, which are used for the dynamic response check. Figure 8(b) shows altitude, dynamic pressure, and altitude rate for the trajectory check.

Roll Requirement

It was desired to be able to roll the vehicle more than $\pm 180^\circ$ and also to have this roll angle displayed to the pilot on the three-axis attitude indicator. The normal approach to this, if the angle were $\pm 180^\circ$ or less, would be simply to drive a servoresolver by the angle, from which the trigonometric functions could be obtained. The attitude indicator would be synchronized with the resolver displaying the same angle. Since the servoresolver is limited to $\pm 180^\circ$, another approach had to be taken. The method of steepest descent was employed to obtain continuous resolution. The equations and programing of this method are shown in figure 9. Five amplifiers and four time-division multipliers are used to solve the equations. This supplies the roll angle for the equations of motion but not for the attitude indicator. To supply the angle ϕ to the attitude indicator, a 10-turn servomultiplier was driven by ϕ with appropriate scaling to give ± 5 revolutions. The attitude indicator was then synchronized with the 10-turn servomultiplier.

Oscilloscope Display

The need for an oscilloscope simultaneously displaying a programed longitudinal acceleration a_x versus climb rate $\dot{h}$, the actual a_x versus $\dot{h}$, and the roll angle ϕ was discussed in a previous section of this text. The mechanization of this display would have been straightforward if three channels were available on the scope. However, only a single beam oscilloscope with dual-channel preamplifiers in both horizontal and vertical inputs was available. Using this oscilloscope alone would have allowed only two variables to be displayed simultaneously. By combining the dual-channel preamplifier oscilloscope with two electronic switches formed by the track and hold facility of the analog computer, all three variables were displayed simultaneously. Figure 10 shows in block form the scope display mechanization used. Electronic switches 3 and 4 are in the pream stage. These were preceded by electronic switches 1 and 2, which were formed by using the track and hold facility. The programed $\dot{h}$ versus a_x is obtained from the function generator being swept by a triangular wave a_x. The angle ϕ is formed by $\overline{A} \cos \phi \sin \omega t$ and $\overline{A} \sin \phi \cos \omega t$.

An important consideration is the proper synchronization of all the switches involved. Switches 1 and 2 are synchronized by having them operated by a common oscillator. This also is true for switches 3 and 4. A synchronized relationship must also exist between switch pairs 1-2 and 3-4 to prevent flicker. Frequencies used successfully for switch pair 1-2, switch pair 3-4, and $\sin \omega t$ were 150 cps triangular wave, 35 cps square wave, and 100 cps sine wave, respectively.

Future Programing Techniques

Through careful programing, the use of electronic components, and the aid of the automatic setup and checkout equipment, an adequate all analog simulation was achieved. However, it became obvious that the analog computer, particularly in the programing of the linear accelerations, was being used to the limit of its capability. It was strongly indicated that it would be advantageous to pursue future simulations of this nature by using "hybrid" computation. A "hybrid" system composed of EAI-231-R consoles and a TRICE, which is a digital differential analyzer, is presently in the checkout stage at the Langley Research Center.

RESULTS AND DISCUSSION

Results of simulations of long range and short range entries are presented and discussed.

Long Range Entries

In performing the long range entries the composite scope presentation of acceleration and rate of climb was utilized as a guidance and situation display.

The control maneuvers used by the pilot in following the nominal curve (fig. 4) are

(1) Hold bank angle of zero through pullout and into skip

(2) Bank to near 90° to hold constant altitude rate of 1,200 fps

(3) Hold bank angle of about 180° to decrease altitude rate as acceleration decreases - that is, the slanted line corresponds to a skipout "warning" boundary, which tells the pilot the acceleration value where his rapid climb must be decreased to avoid uncontrollable skipouts

(4) Hold bank angle of approximately 90° or 270° to maintain constant altitude rate of 600 ft/sec

(5) As acceleration decreases, bank angle is gradually brought to 0° bank angle to maintain the altitude rate of 600 ft/sec

To improve the accuracy of altitude-rate data, a 3:1 scale change was incorporated at low acceleration during the time the pilot held a climb rate of 600 ft/sec. This scale change was necessary because of the sensitivity of maximum altitude and range in the skipping maneuver to the vehicle altitude rate at exit from the atmosphere. In fact, control of this skipout altitude rate could be used to vary final range.

After the high altitude skip was completed and the vehicle again descended into denser atmosphere, a terminal guidance task was employed to control the vehicle to the desired touchdown point. This task consisted of following an equilibrium glide trajectory which was presented on an X-Y plotter. The reference trajectory used is shown in figure 11(a) and corresponds to a terminal glide at an L/D of 0.3. The spacecraft, possessing an L/D of 0.5, thus has a capability for being controlled to the reference trajectory from either side of it.

Results of two piloted entries are shown in figure 11. Data presented are the variations with downrange of altitude, crossrange, acceleration, roll attitude, and angle of attack. Regardless of automatic damper condition the pilot did a good job of navigating to the destination. (Note that all reentries were terminated at an altitude of 100,000 feet, the limit accepted for analog scaling.) The bank-angle curve shows the maneuvers required to complete the downrange task with no resultant crossrange. For both damper conditions, the final crossrange was small. With dampers out the pilot was not often able to completely damp vehicle angular motions and much of his attention was required, both in and out of the atmosphere, in monitoring and controlling attitude. The angle-of-attack plot illustrates two types of corrective control measures required of the pilot with dampers out. Out of the atmosphere, small pitch rates caused the angle of attack to slowly drift off from the trim value of -33° and the pilot periodically introduced control inputs in the opposite direction when the deviations became large. As the vehicle reentered the atmosphere, the pilot would reestablish the trim angle of attack. Within the atmosphere it was necessary for the pilot to monitor and occasionally damp, by control inputs, transient motions in both angle of attack (shown in fig. 11(b)) and sideslip (not illustrated). As a result of

this demand on the pilot's attention and the consequently reduced attention he could devote to the navigational task, the all-dampers-out condition was rated unacceptable for normal operation.

Short Range Entries

For entries in which short range was desired, no guidance was used but the pilot was given the task of maintaining a constant 6g deceleration. To accomplish such runs, quickened acceleration $\left[a_x + K\frac{d(a_x)}{dt}\right]$ and vehicle bank angle were displayed on the oscilloscope. This required only minor modifications of the scope presentation used for long range entries. The merits of quickening as a pilot aid in controlling attitude are well established, and in this trajectory task the pilot was able to maintain a constant acceleration only when quickened acceleration was displayed. Results of entries with dampers in and out are shown in figure 12. For both damper conditions safe entries were accomplished, the main difference being the lack of precision in controlling acceleration with all dampers out.

Minimum Display

Of interest from simplicity and emergency considerations are the minimum display instruments required for a safe entry through the atmosphere, in which no navigation is attempted. With stability augmenters operative, the pilots were able to make safe entries with only bank attitude and longitudinal acceleration displayed. The results corroborate those reported by other investigators (ref. 5). Figure 13 shows some results for both a shallow entry and a steep entry, in which the pilot task was to maintain 2g.

For the shallow entry the pilot inverts the spacecraft (directs lift downward) until a 2g condition is reached. From here he controls the bank angle as necessary to maintain 2g. For this condition no attempt is made to control the crossrange.

For the steep entry the 10g condition is reached at pullout and a shallow climb is performed by the pilot, the acceleration gradually leveling off to the 2g condition. The range traveled in the steep entry is less than that for the shallow entry because of a higher acceleration (maximum of 10g) environment.

CONCLUDING REMARKS

A piloted earth reentry at parabolic velocity was satisfactorily simulated through the use of analog computing equipment. The results of the simulation study indicated that maneuvers required for long-range navigation tasks could be accomplished with or without damping augmentation by using simple navigation displays; short range entries could be accomplished with or without damping augmentation when the pilot was presented a quickened acceleration signal for control;

and safe entries could be performed from either a shallow or steep entry condition with a display presentation of only bank angle and longitudinal acceleration, the technique being to establish and maintain a constant acceleration condition.

APPENDIX A

SYMBOLS

A	flight-path heading angle
a	acceleration resulting from aerodynamic forces
C_l	rolling-moment coefficient
C_m	pitching-moment coefficient
C_n	yawing-moment coefficient
C_X	longitudinal-force coefficient
C_Y	side-force coefficient
C_Z	normal-force coefficient
$C_{Y_\beta}, C_{n_\beta}, C_{l_\beta}, C_{Z_\alpha}$ $C_{m_q}, C_{n_r}, C_{l_p}$	aerodynamic derivatives
d	capsule diameter
G	gain
g	acceleration due to gravity
h	altitude
I_X	moment of inertia about body X-axis
I_Y	moment of inertia about body Y-axis
I_Z	moment of inertia about body Z-axis
I_{XZ}	product of inertia
K	gain in quickened acceleration
L	longitude
L/D	lift-drag ratio

$$L_p = \frac{\bar{q}Sd^2}{2V} C_{l_p}$$

$$L_\beta = \bar{q}SdC_{l_\beta}$$

l,m,n

l_1, l_2, l_3

m_1, m_2, m_3

n_1, n_2, n_3

direction cosines

$$M_q = \frac{\bar{q}Sd^2}{2V} C_{m_q}$$

$$(M)_\alpha = \bar{q}SdC_m$$

$$N_r = \frac{\bar{q}Sd^2}{2V} C_{n_r}$$

$$N_\beta = \bar{q}SdC_{n_\beta}$$

m	vehicle mass
M	pilot control moment
p,q,r	vehicle angular velocity about X-, Y-, and Z-axis, respectively
$\bar{q}$	dynamic pressure
r	vehicle distance from center of earth
S	capsule cross-sectional area
t	time
u,v,w	velocity component along body X-, Y-, and Z-axis, respectively
V	vehicle velocity
X,Y,Z	right-hand Cartesian axis system
α	angle of attack
β	angle of sideslip
γ	flight-path angle

λ	latitude
ρ	atmosphereic density
ψ, θ, ϕ	Euler angles relating body axes to geographic axes
ω	forcing frequency

Subscripts:

x,y,z	vector components along respective axes
o	initial condition

A dot over a symbol indicates a derivative with respect to time.

APPENDIX B

EQUATIONS OF MOTION

Equations defining the angular and translatory motions of the spacecraft are given herein. Moment equations are written in a body axes system and translation equations are written in a geographic axes system in which the X-axis coincides with the horizontal component of the initial velocity vector. Assumptions pertinent to the equations are

(1) Axes system fixed to center of earth defines an inertial set

(2) Earth is spherical and nonrotating

(3) Acceleration due to gravity is considered constant

(4) Out-of-plane velocity V_y and displacement λ are small such that $\tan \lambda \approx \lambda$.

The following translation equations are obtained from the classical equations in spherical coordinates (for example, p. 51 of ref. 6) by introducing the assumptions for V_y and λ and neglecting higher order terms:

Translation equations in geographic axes system:

$$\dot{V}_x = l_1 a_x + m_1 a_y + n_1 a_z + \frac{V_x V_z}{r}$$

$$\dot{V}_y = l_2 a_x + m_2 a_y + n_2 a_z - \frac{V_x^2 \lambda}{r}$$

$$\dot{V}_z = l_3 a_x + m_3 a_y + n_3 a_z + g - \frac{V_x^2}{r}$$

Moment equations in body axes system:

$$I_X \dot{p} - (I_Y - I_Z)qr - I_{XZ}\dot{r} - I_{XZ}pq = L_p p + L_\beta \beta + M_x$$

$$I_Y \dot{q} - (I_Z - I_X)pr - I_{XZ}r^2 + I_{XZ}p^2 = M_q q + (M)_\alpha + M_y$$

$$I_Z \dot{r} - (I_X - I_Y)pq - I_{XZ}\dot{p} + I_{XZ}qr = N_r r + N_\beta \beta + M_z$$

Euler angle rate equations:

$$\dot{\phi} = p + q \sin \phi \tan \theta + r \cos \phi \tan \theta$$

$$\dot{\theta} = q \cos \phi - r \sin \phi + \dot{L} \cos \psi$$

$$\dot{\psi} = r \frac{\cos \phi}{\cos \theta} + q \frac{\sin \phi}{\cos \theta}$$

Aerodynamic forces:

$$a_x = \frac{\bar{q}S}{m} C_X$$

$$a_y = \frac{\bar{q}S}{m} C_{Y_\beta} \beta$$

$$a_z = \frac{\bar{q}S}{m} C_Z$$

Aerodynamic relations:

$$\begin{bmatrix} u \\ v \\ w \end{bmatrix} = \begin{bmatrix} l_1 & l_2 & l_3 \\ m_1 & m_2 & m_3 \\ n_1 & n_2 & n_3 \end{bmatrix} \begin{bmatrix} V_x \\ V_y \\ V_z \end{bmatrix}$$

$$\tan \alpha = \frac{w}{u}$$

$$\gamma = - \frac{V_z}{V}$$

$$\bar{q} = \frac{1}{2} \rho V^2$$

$$\beta = \frac{v}{V}$$

$$A = \frac{V_y}{V_x}$$

Position data:

$$\dot{L} = \frac{V_x}{r}$$

$$\dot{\lambda} = \frac{V_y}{r}$$

$$\dot{h} = -V_z$$

Vehicle control system:

Control moment inputs are the sum of pilot-applied moments and automatic damper inputs. These equations are

$$\frac{M_x}{I_X} = \dot{p}_s - k_p p$$

$$\frac{M_y}{I_Y} = \dot{q}_s - k_q q$$

$$\frac{M_z}{I_z} = \dot{r}_s - k_r r$$

where k_p, k_q, k_r are constant damper gains and $\dot{p}_s$, $\dot{q}_s$, $\dot{r}_s$ are pilot inputs. Limits are placed on $\frac{M_x}{I_X}$, $\frac{M_y}{I_Y}$, $\frac{M_z}{I_Z}$, $\dot{p}_s$, $\dot{q}_s$, $\dot{r}_s$.

REFERENCES

1. Chapman, Dean R.: An Analysis of the Corridor and Guidance Requirements for Supercircular Entry Into Planetary Atmospheres. NASA TR R-55, 1960.

2. Becker, J. V., Baradell, D. L., and Pritchard, E. B.: Aerodynamics of Trajectory Control for Re-Entry at Escape Speed. Astronautica Acta, Vol. VII, Fasc. 5-6, 1961, pp. 334-358.

3. Isakson, Gabriel: Flight Simulation of Orbital and Reentry Vehicles. Part I - Development of Equations of Motion in Six Degrees of Freedom. ASD TR 61-171 (I), Oct. 1961.

4. Fogarty, L. E., and Howe, R. M.: Flight Simulation of Orbital and Reentry Vehicles. Part II - A Modified Flight Path Axis System for Solving the Six-Degree-of-Freedom Flight Equations. ASD TR 61-171 (II), Oct. 1961.

5. Young, John W., and Barker, Lawrence E., Jr.: Moving-Cockpit-Simulator Study of Piloted Entries Into the Earth's Atmosphere for a Capsule-Type Vehicle at Parabolic Velocity. NASA TN D-1797, 1963.

6. Page, Leigh: Introduction to Theoretical Physics. Second ed., D. Van Nostrand Co., Inc., 1935.

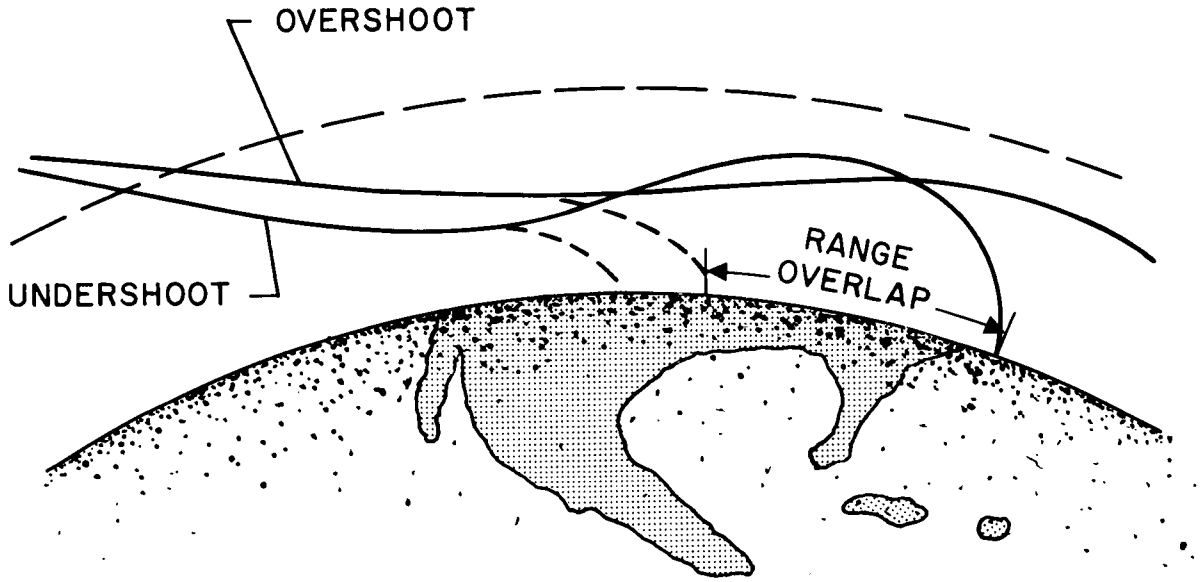

NASA

Figure 1.- Long and short range earth entries at parabolic velocity.

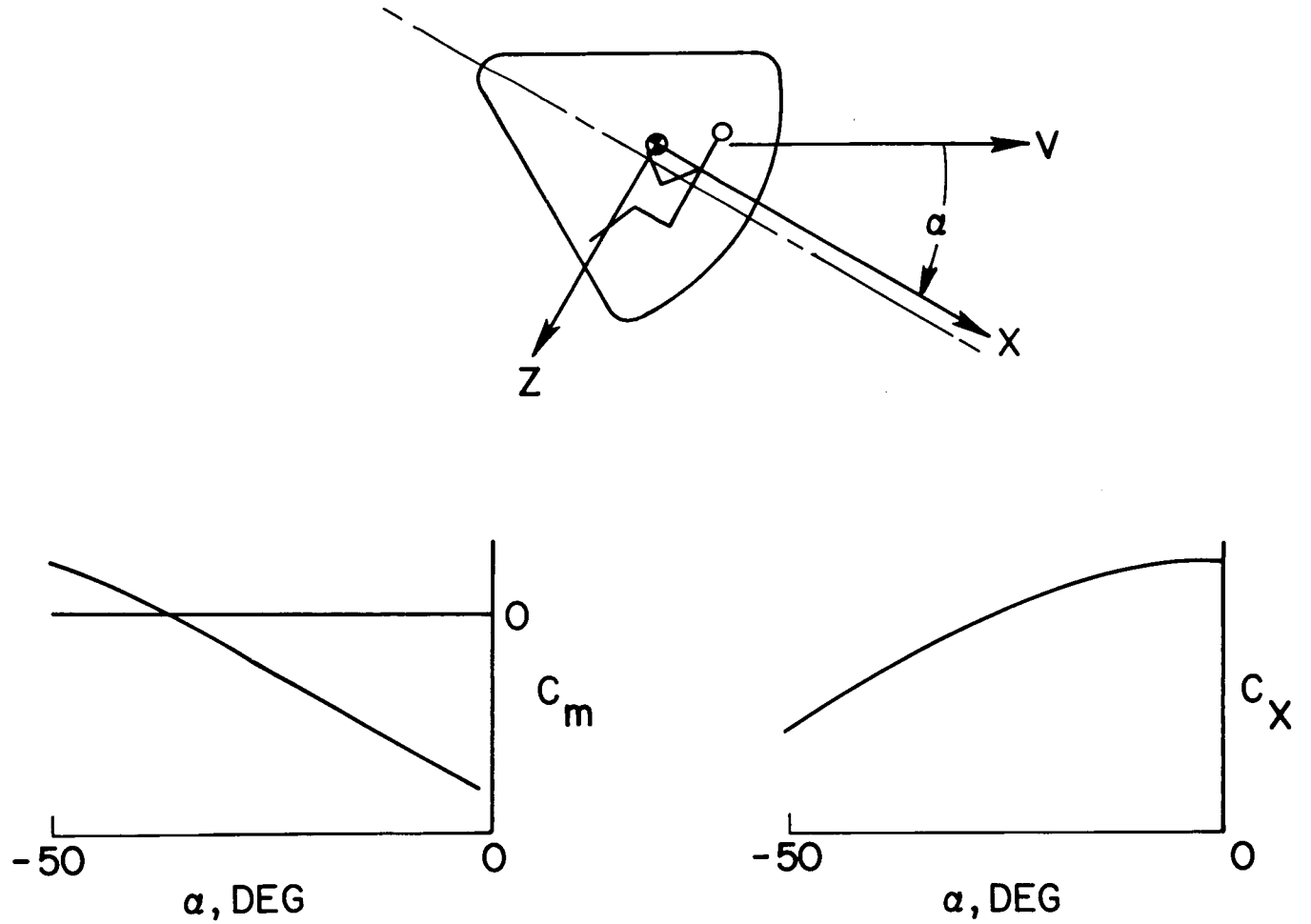

Figure 2.- Vehicle configuration and aerodynamic characteristics.

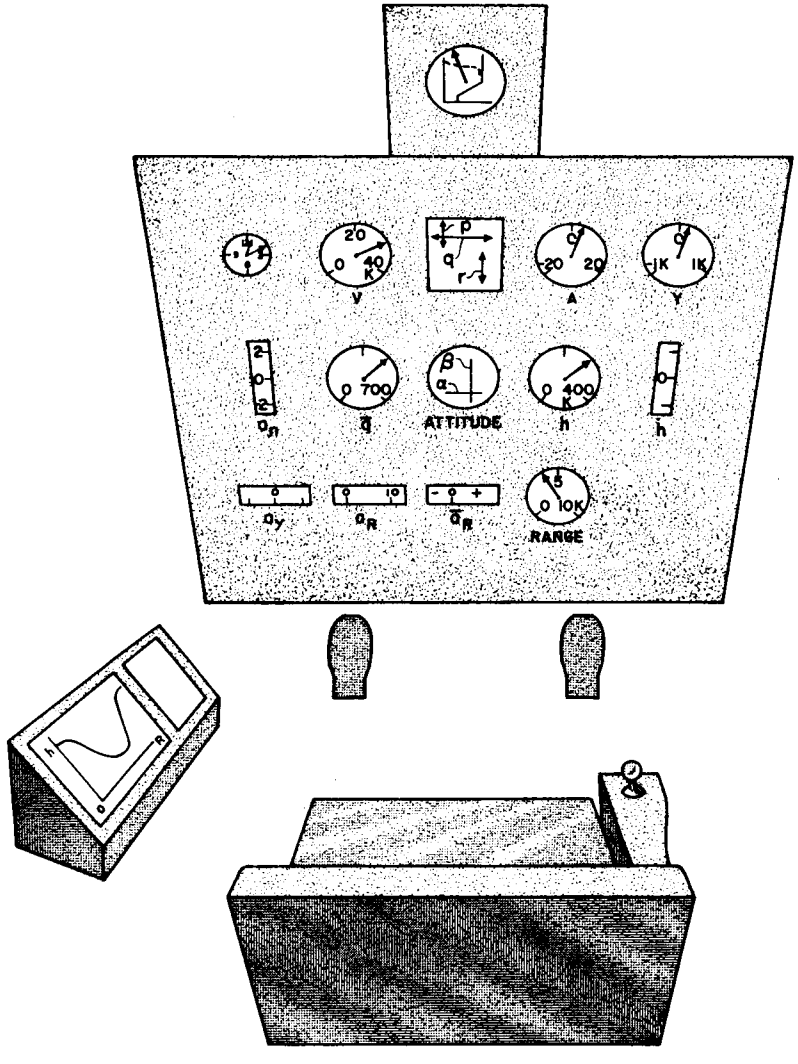

NASA

Figure 3.- Pilot station and instrument display.

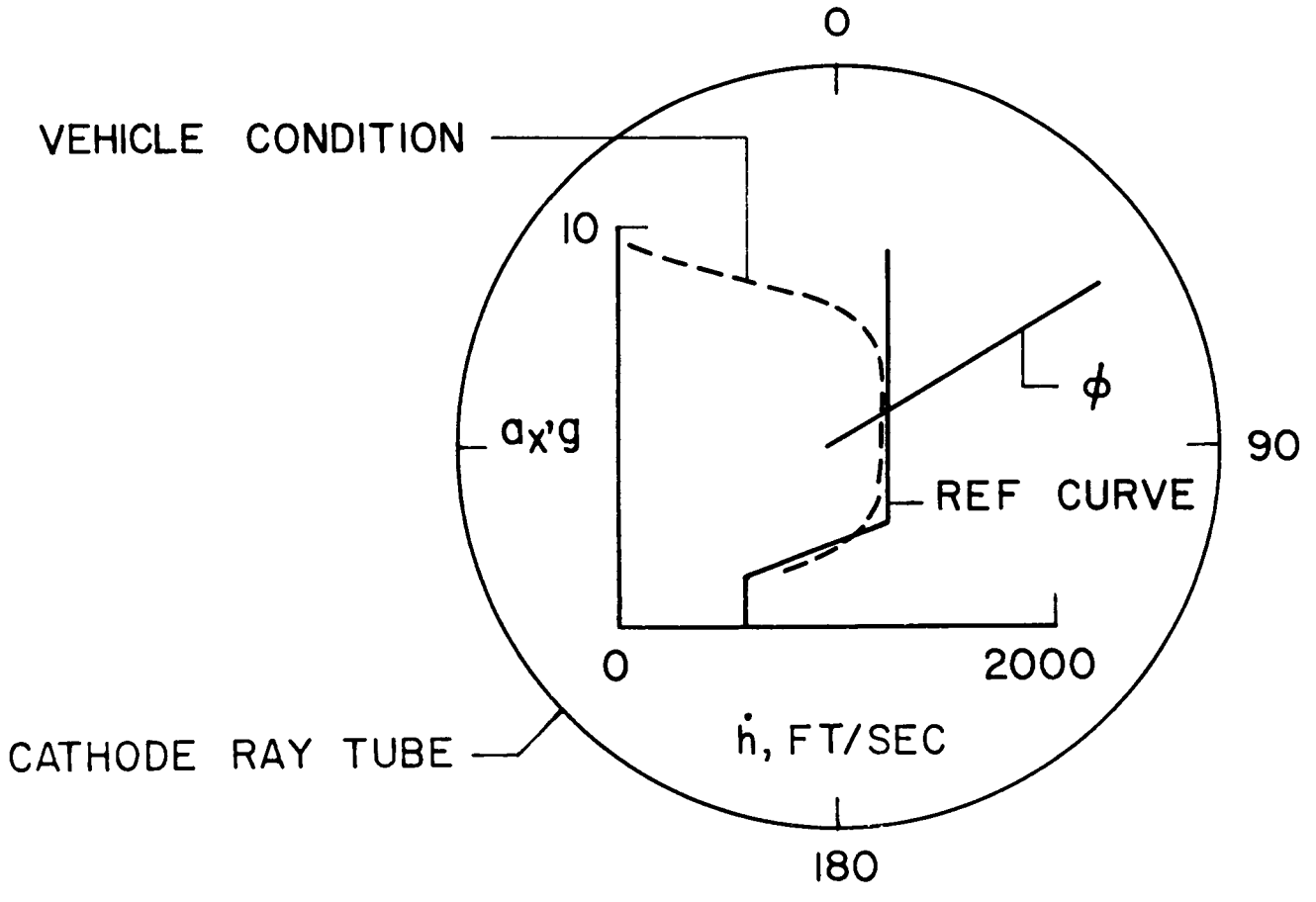

Figure 4.- Trajectory guidance and situation display.

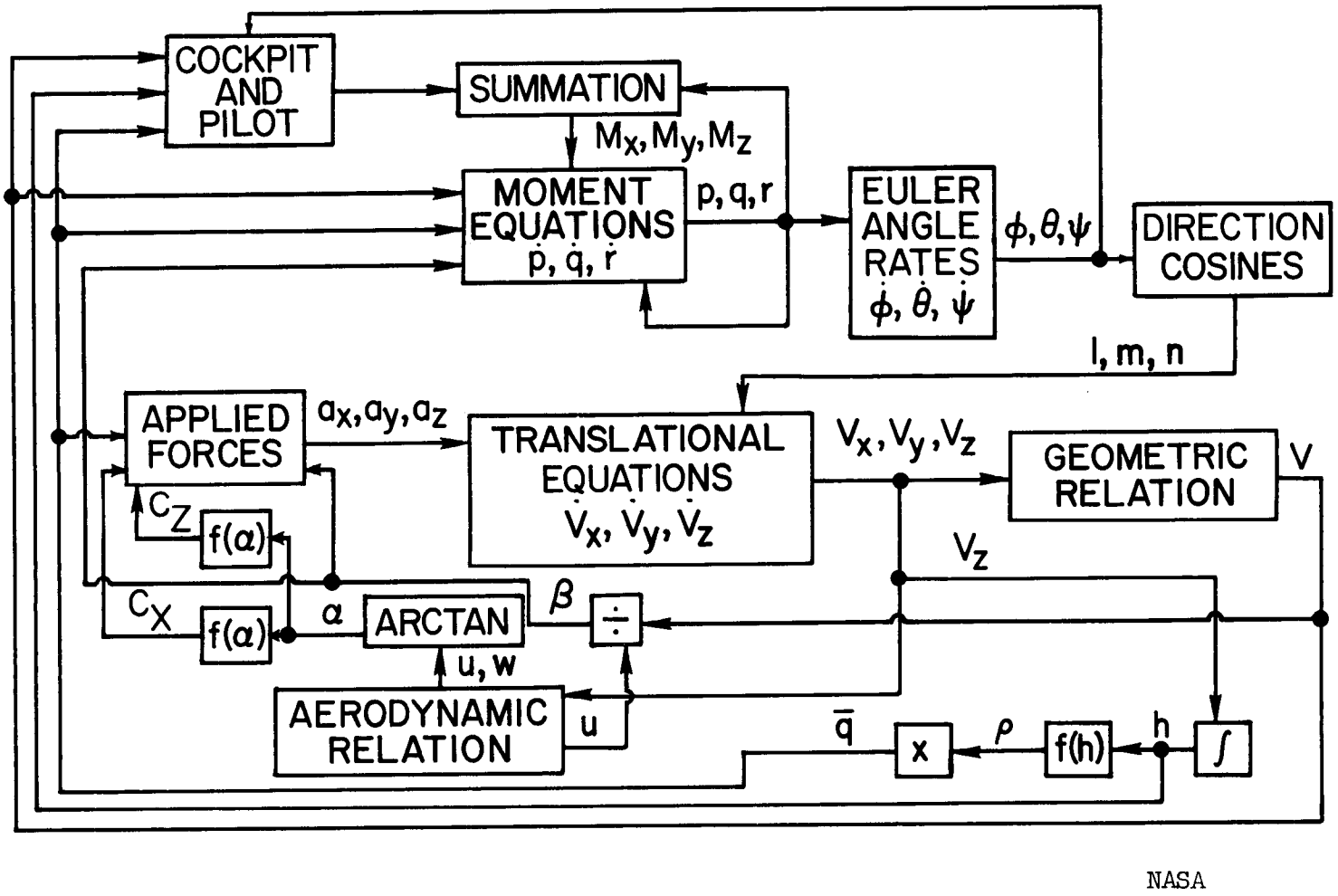

NASA

Figure 5.- General block diagram of reentry simulation.

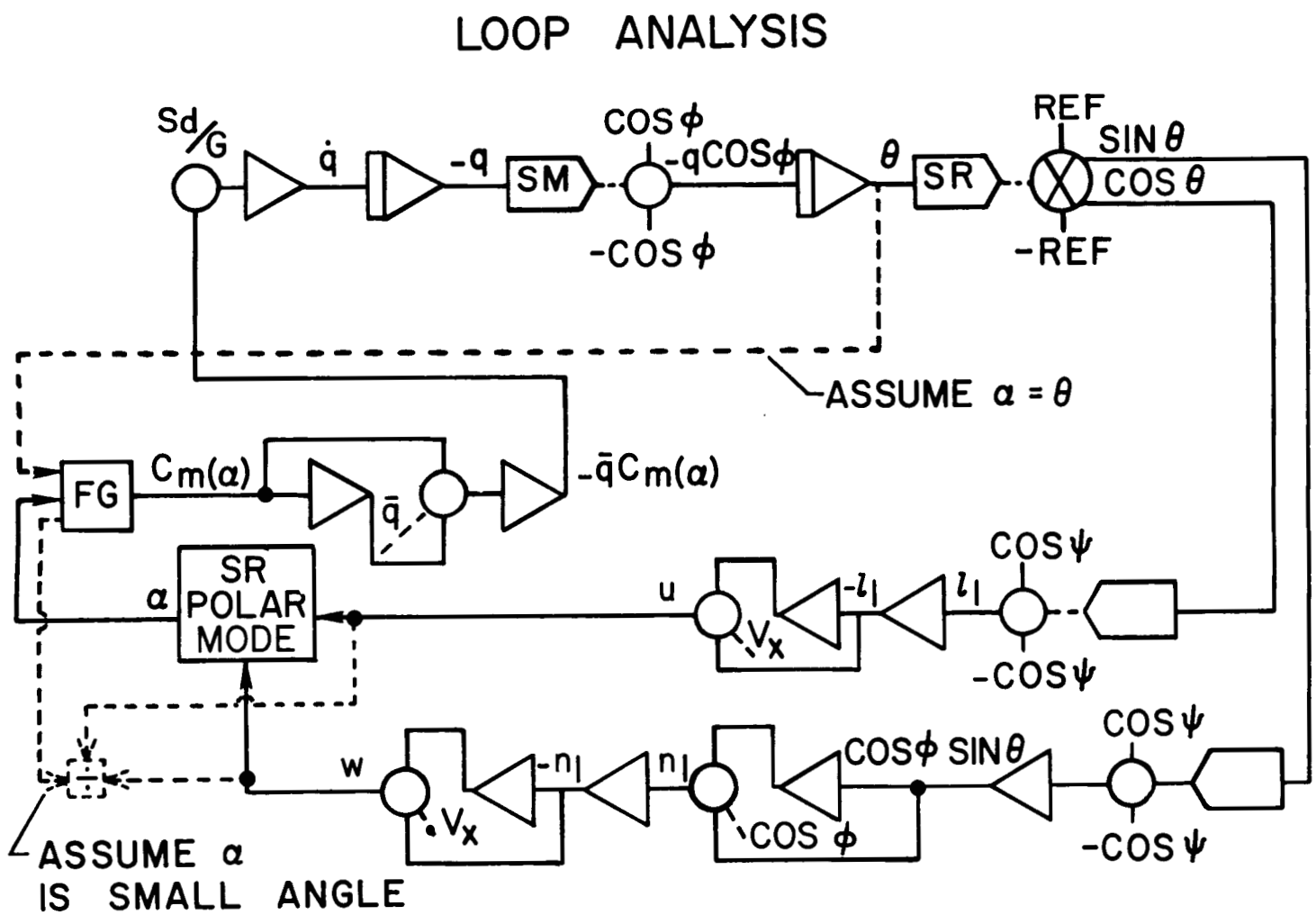

Figure 6.- Loop analysis.

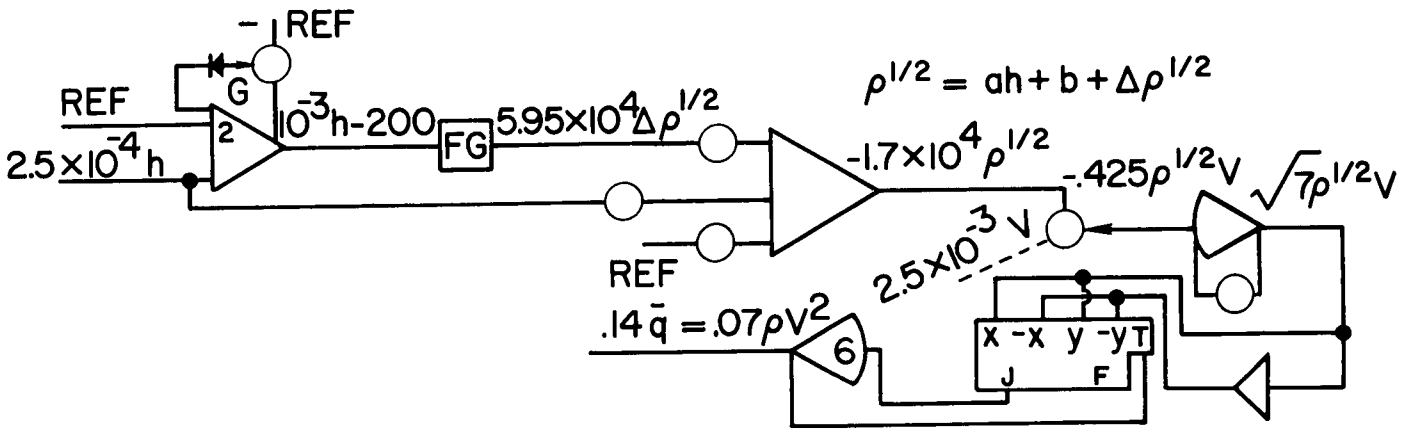

NASA

Figure 7.- Programing of dynamic pressure.

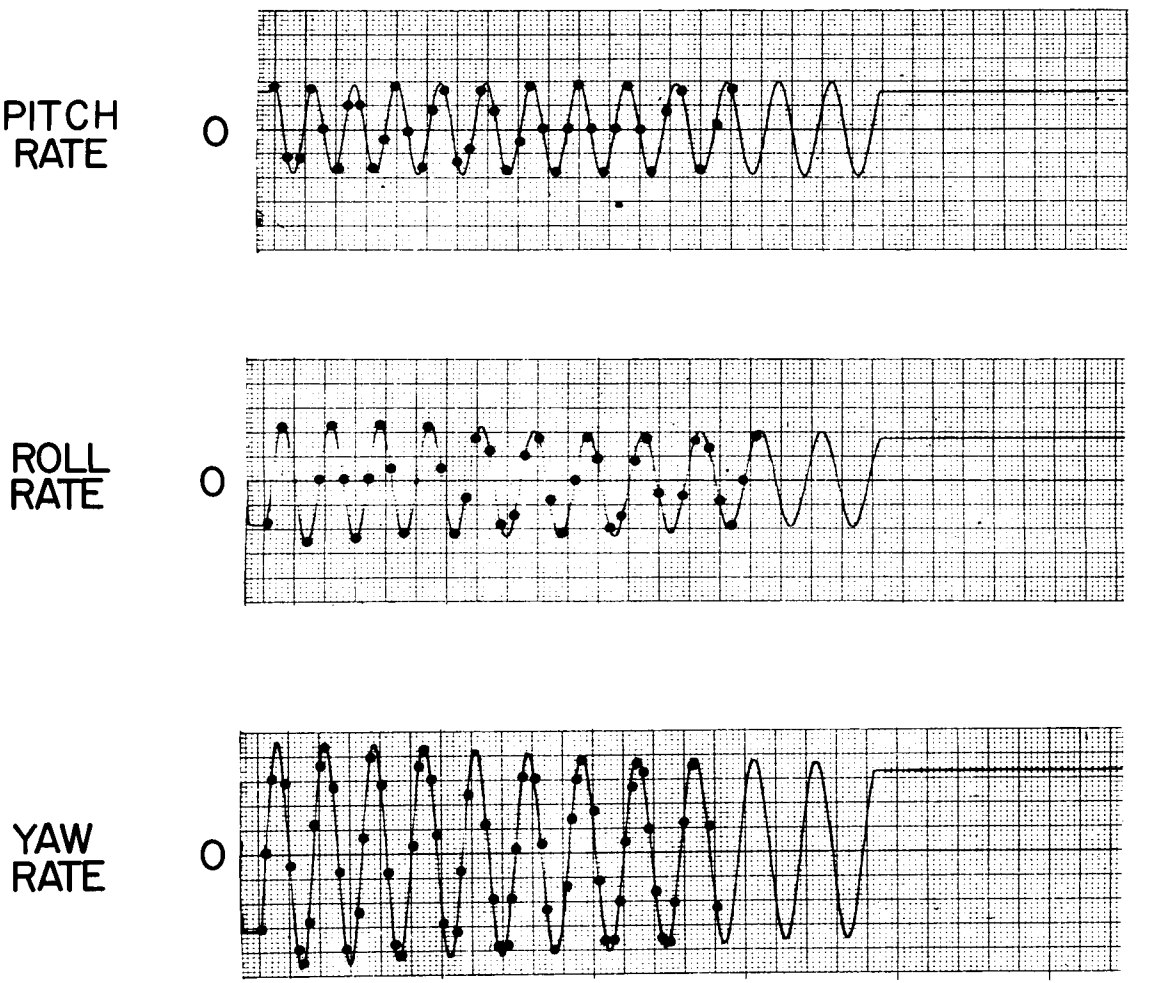

Figure 8a.- Combined longitudinal and lateral response check.

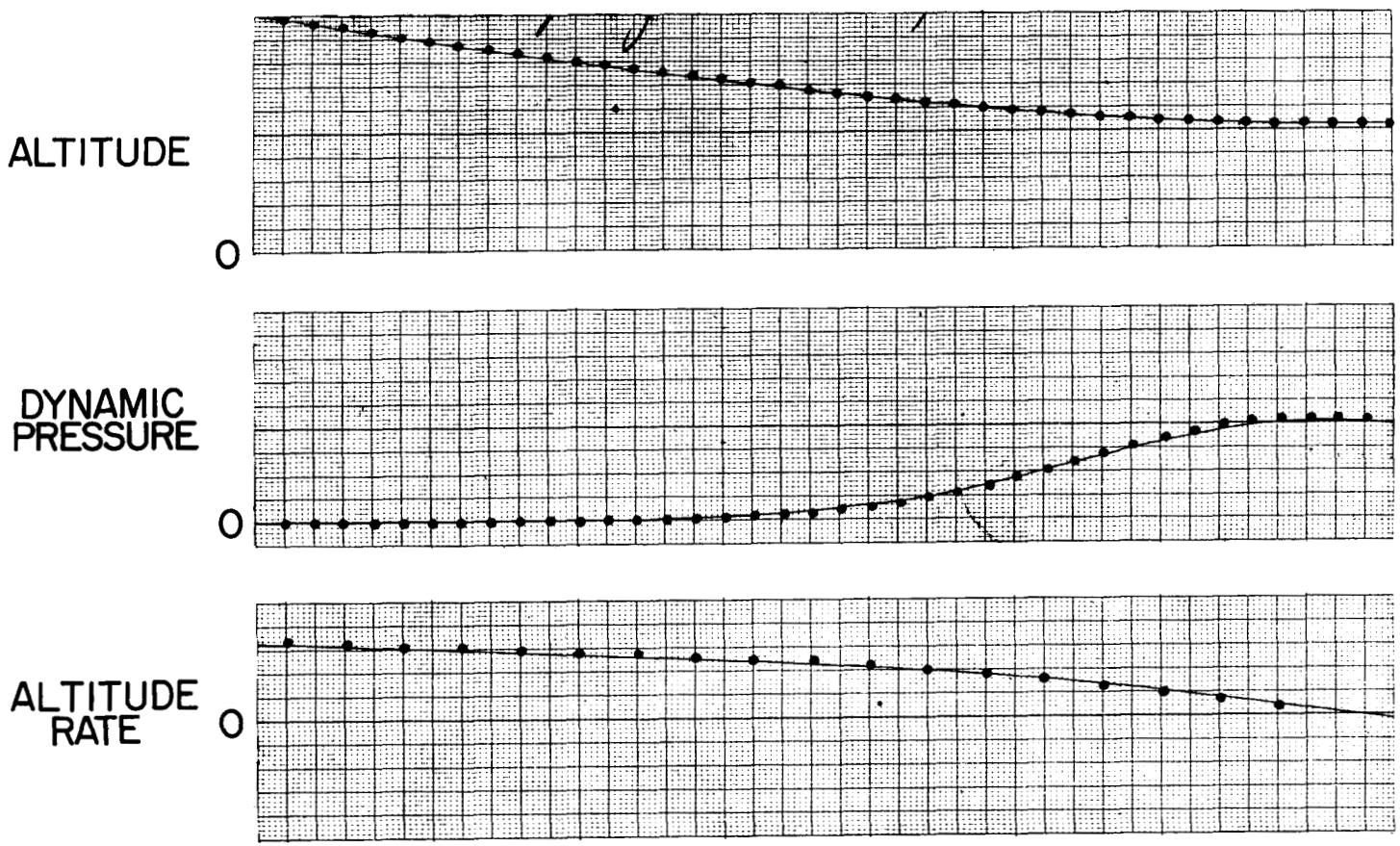

Figure 8b.- Trajectory check.

$$\text{SIN}\ \phi = \int \left[\dot{\phi}\ \text{COS}\ \phi - k\epsilon \frac{\partial \epsilon}{\partial\ \text{SIN}\phi} \right] dt \qquad \frac{\partial \epsilon}{\partial\ \text{SIN}\phi} = 2\ \text{SIN}\phi$$

$$\text{COS}\ \phi = \int \left[-\dot{\phi}\ \text{SIN}\theta - k\epsilon \frac{\partial \epsilon}{\partial \text{COS}\phi} \right] dt \qquad \frac{\partial \epsilon}{\partial \text{COS}\phi} = 2\ \text{COS}\phi$$

$$\epsilon = \text{SIN}^2\phi + \text{COS}^2\phi - 1$$

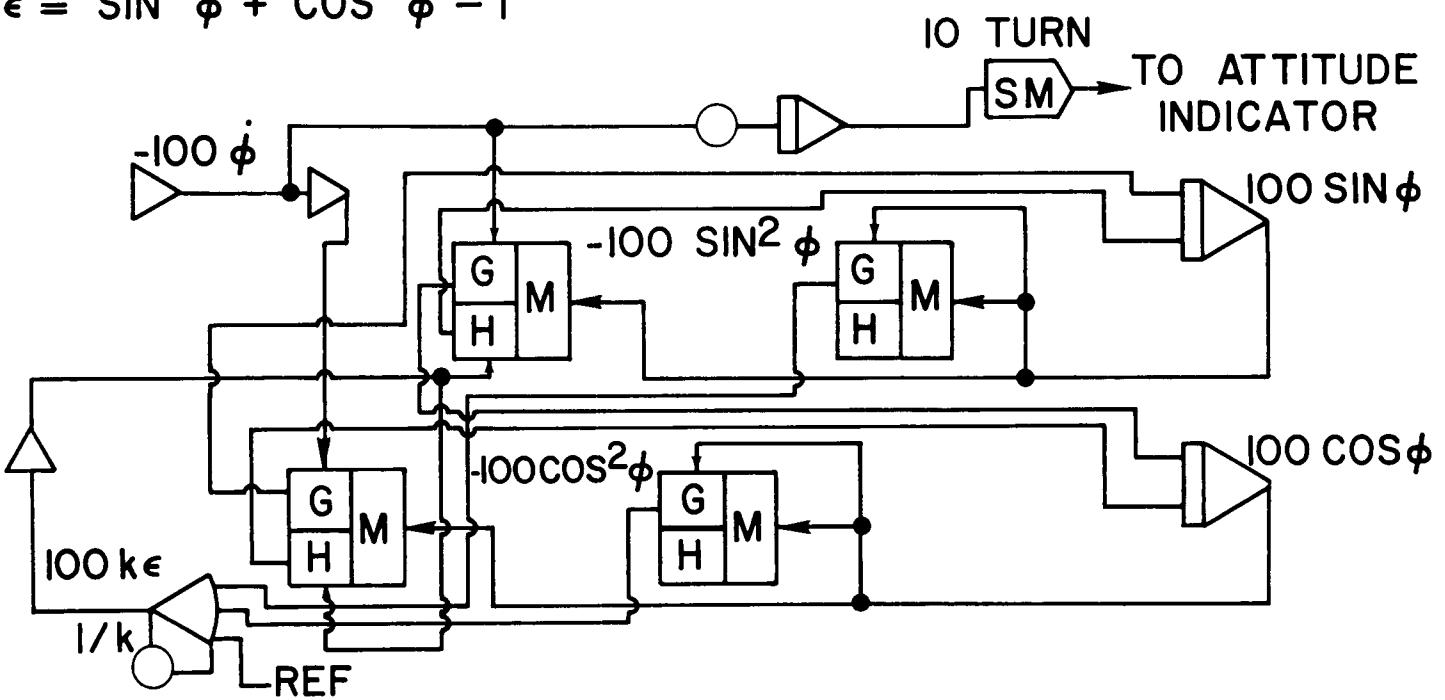

NASA

Figure 9.- Method of steepest descent.

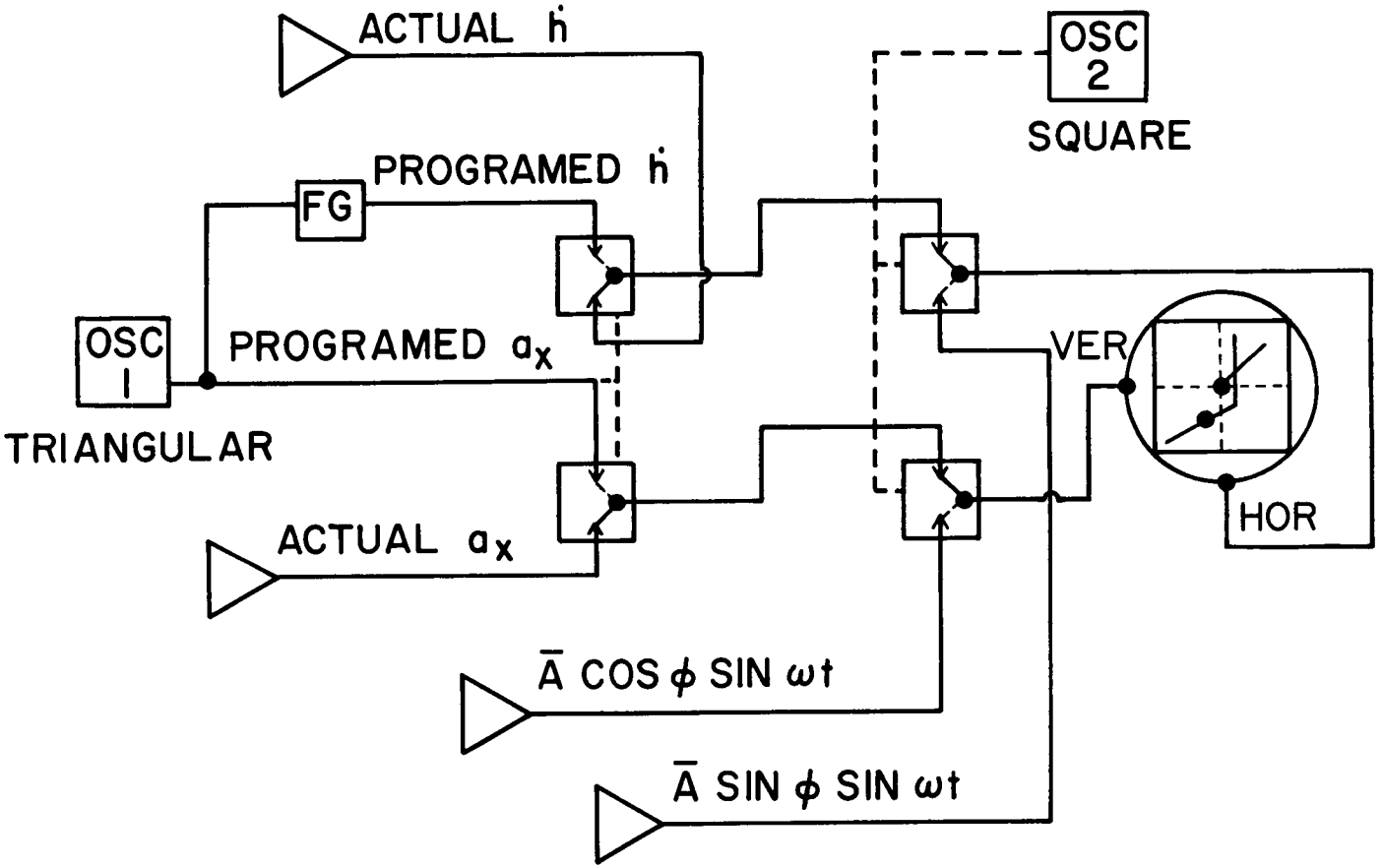

Figure 10.- Circuitry for scope display.

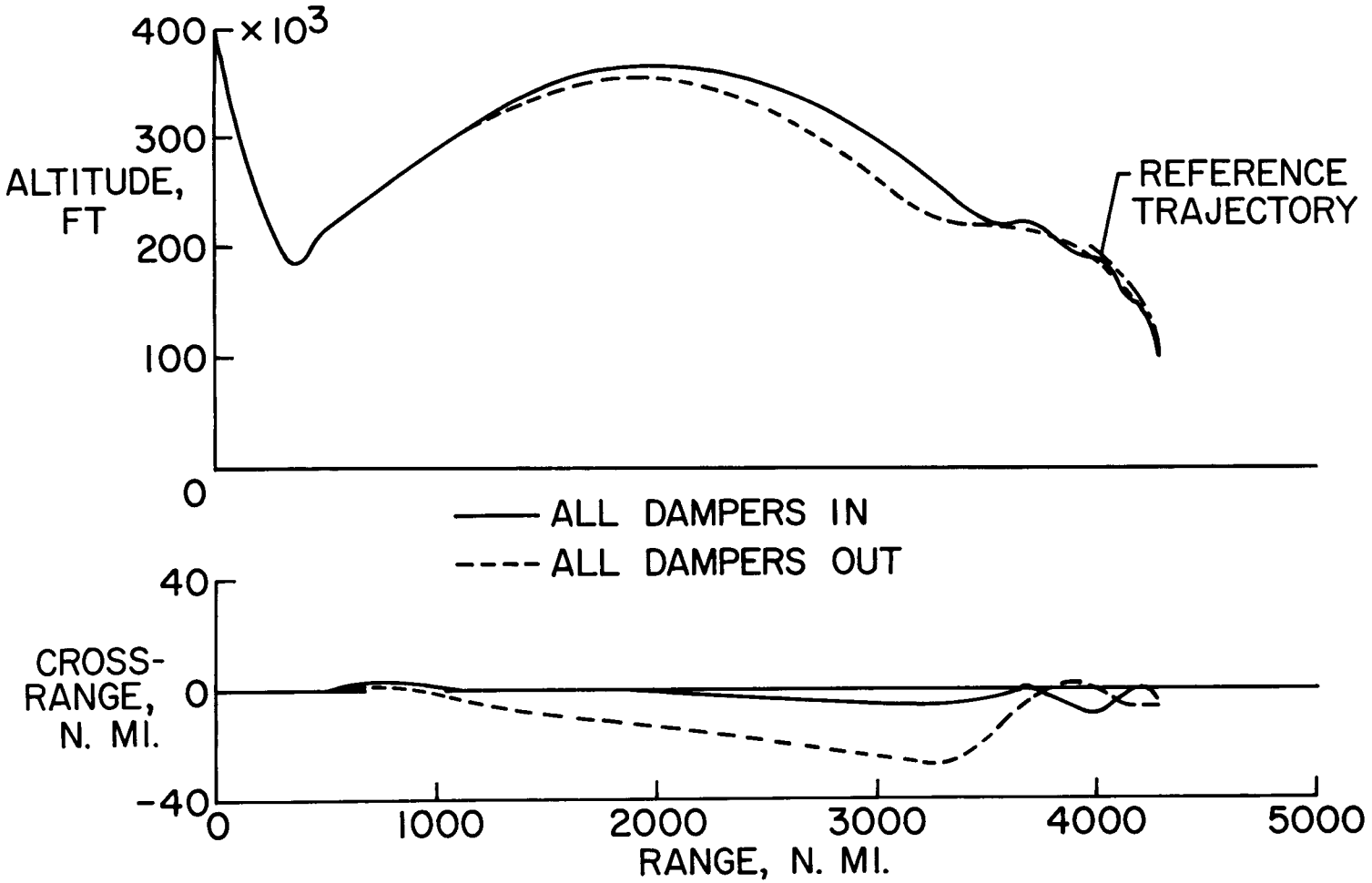

(a) Altitude and crossrange histories. NASA

Figure 11.- Effect of automatic damper condition on long range entries.

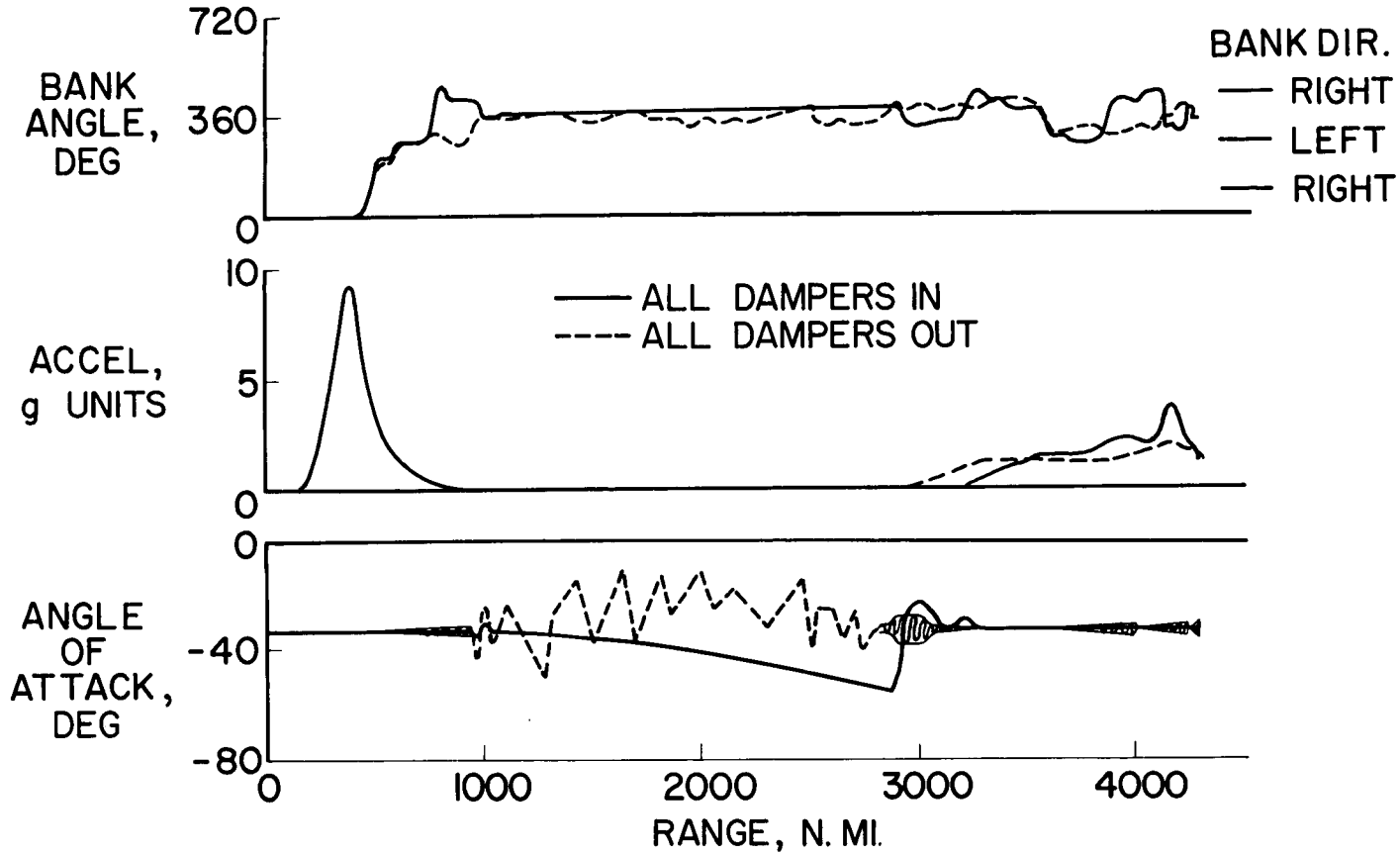

(b) Bank angle, acceleration, and angle-of-attack histories. NASA

Figure 11.- Concluded.

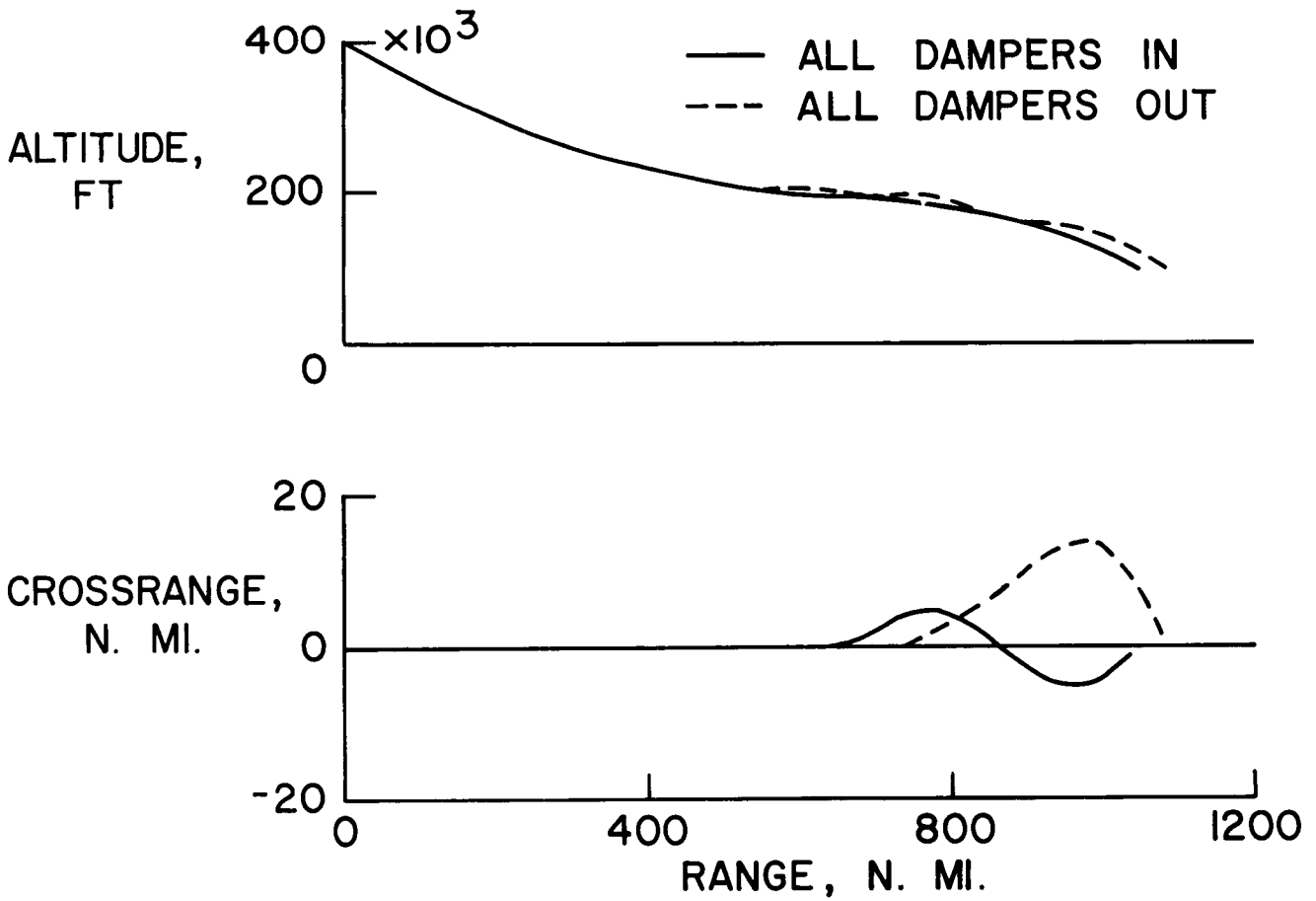

(a) Altitude and crossrange histories. NASA

Figure 12.- Effect of automatic damper condition on short range entries.

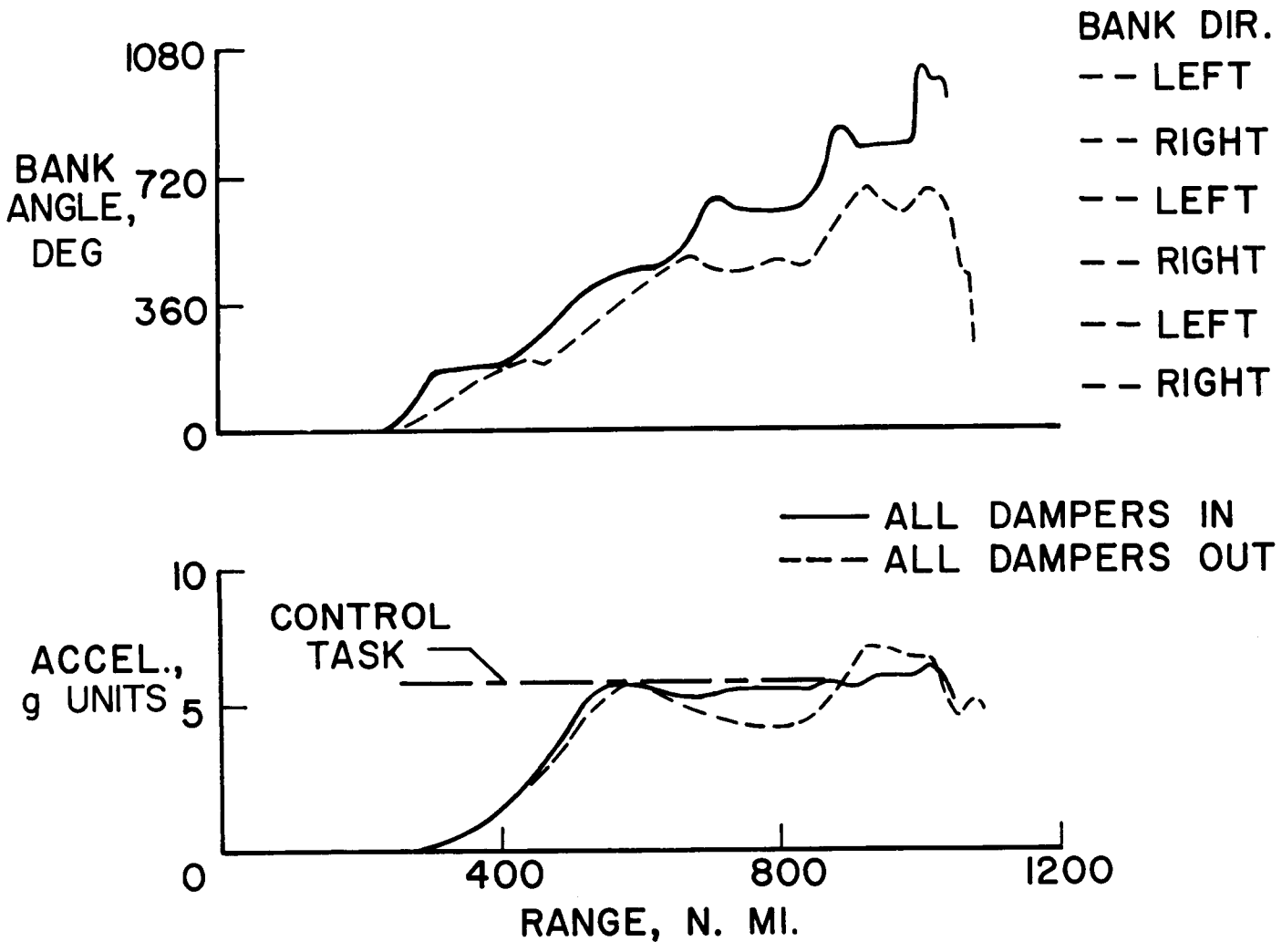

(b) Bank angle and acceleration histories. NASA

Figure 12.- Concluded.

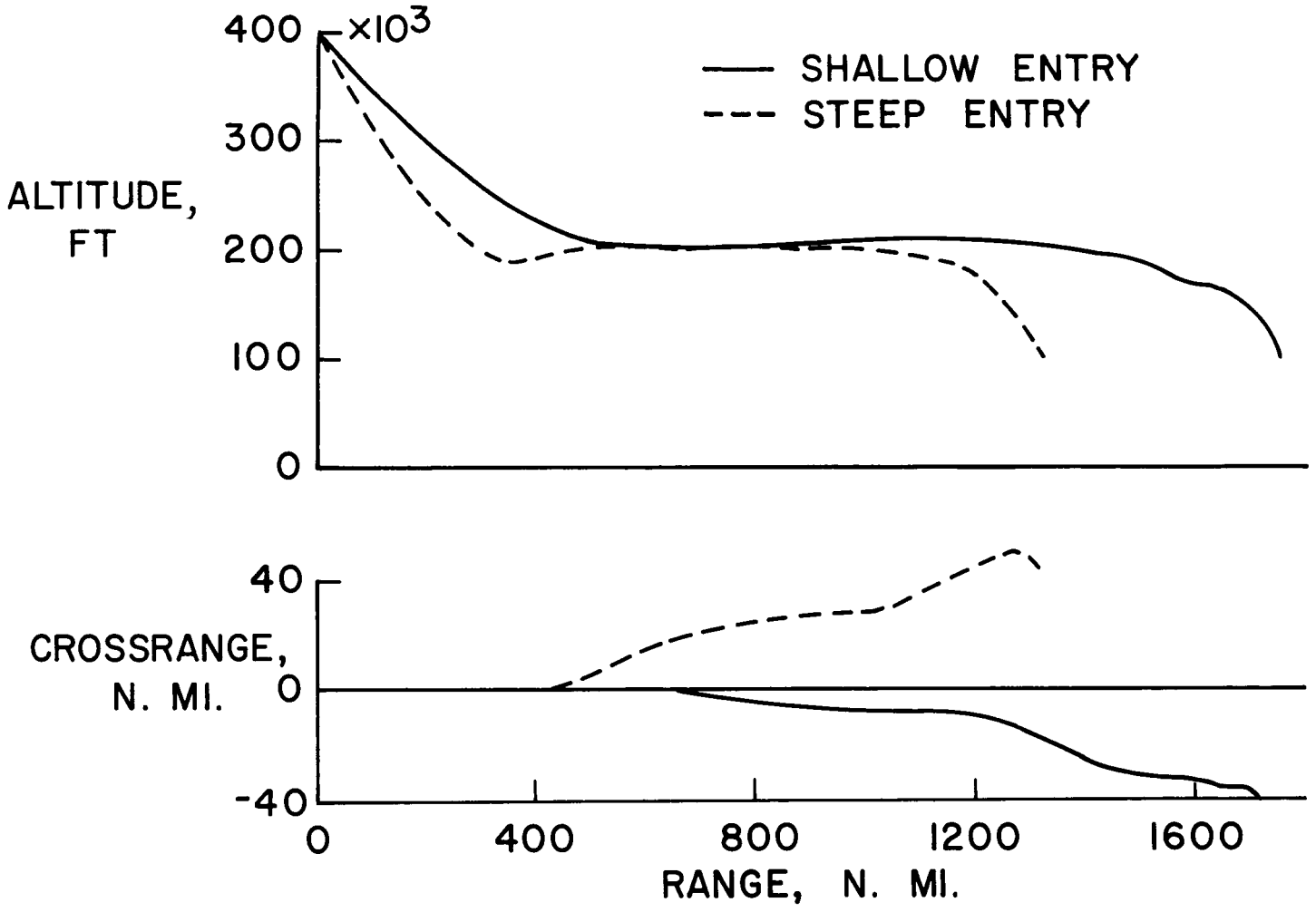

(a) Altitude and crossrange histories. NASA

Figure 13.- Effect of entry angle on entries with minimum display instrumentation.

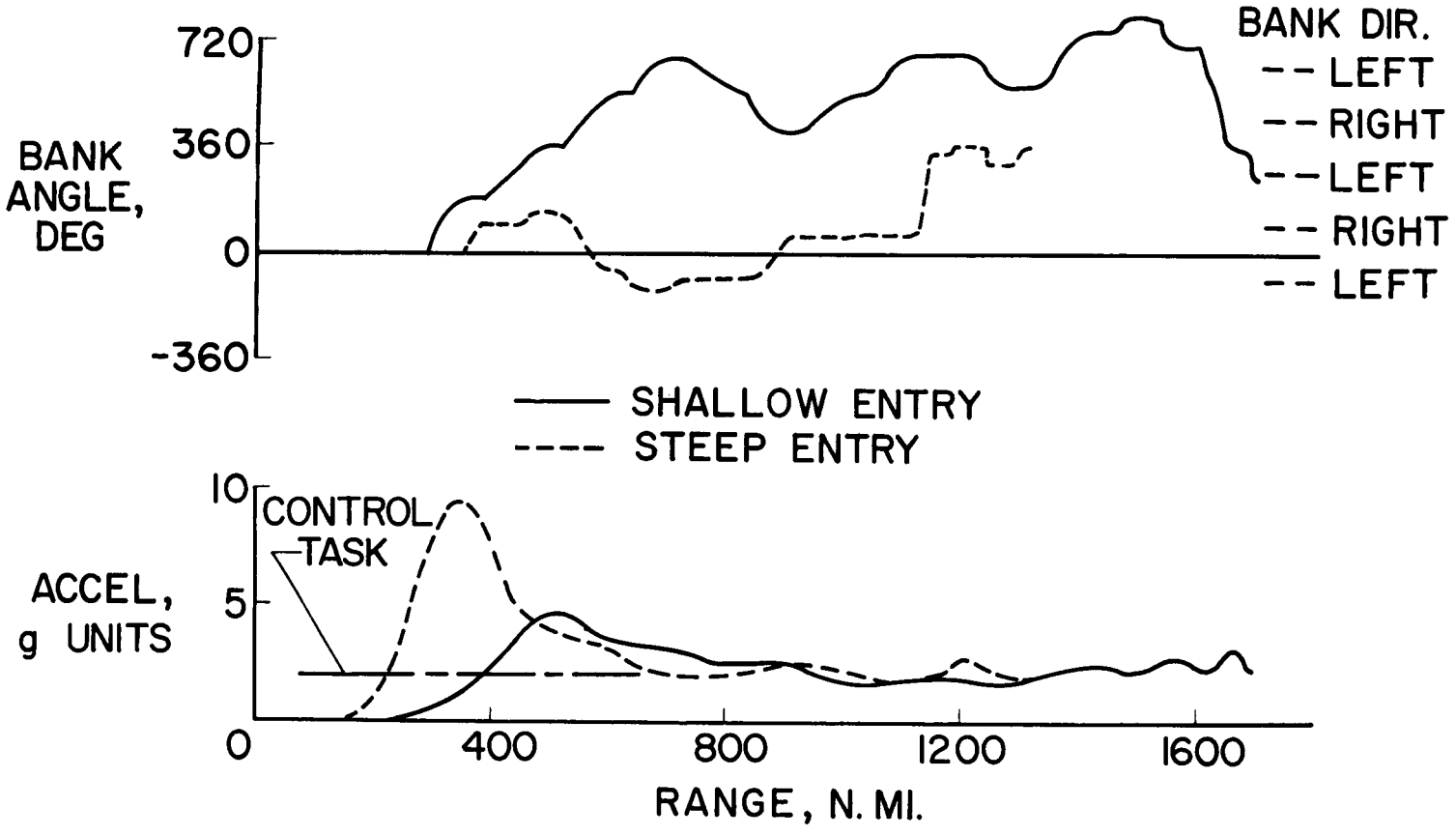

(b) Bank angle and acceleration histories. NASA

Figure 13.- Concluded.